SUPPORTING INFORMATION: Titanium Contacts to Graphene: Process-Induced Variability in Electronic and Thermal Transport

Keren M. Freedy[1], Ashutosh Giri[2], Brian M. Foley[2], Matthew R. Barone[1], Patrick E. Hopkins[1,2], Stephen McDonnell[1]

[1]Department of Materials Science and Engineering, University of Virginia, Charlottesville, Virginia, 22904, United States

[2]Department of Mechanical and Aerospace Engineering, University of Virginia, Charlottesville, Virginia, 22904, United States

KEYWORDS: Graphene, Vacuum Deposition, Contact Resistance, Thermal Boundary Conductance, X-ray Photoelectron Spectroscopy, Thermal Transport, Interface Chemistry

CORRESPONDING AUTHOR: mcdonnell@virginia.edu.

Characterization of Starting Material

The experiments in this work utilized a 4"x4" sheet of CVD-grown graphene on Cu purchased from Graphene Supermarket. Elemental analysis with XPS shows the presence of Cu, C, and O on the Gr/Cu material prior to transfer. Following transfer of Gr to SiO_2, XPS shows Si, C, and O. To characterize spot-to-spot variability in the starting material we have acquired Raman line scans of ~10 spots across a ~200 μm line at different regions of the 4"x4" Gr/Cu sheet. A laser wavelength of 405 nm was used. The average of four sets of 10 spectra are shown below in Figure S1. The corresponding data for each spectrum is summarized in Table S1 and indicates reasonable uniformity across the sample.

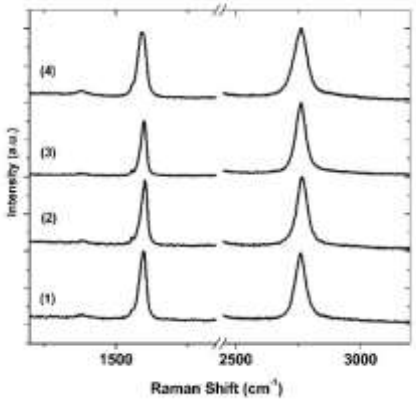

Figure S1. Raman spectra representing the average of 10 spots per line of length ~200 μm at four macroscopically different regions of the Gr/Cu starting material.

Table S1: Spectral Features of Starting Material

Region	D/G Ratio	G/2D Ratio	D Position	G Position	2D Position
1	0.22	1.15	1378	1592	2760
2	0.23	0.94	1375	1598	2765
3	0.16	0.84	1376	1596	2760
4	0.27	1.02	1380	1591	2761

Graphene Transfer Process

The starting material (Graphene Supermarket 4"x4" Gr/Cu) was cut into ~2x2 cm pieces for transfer onto 300 nm SiO_2/Si purchased from University Wafer. A solution of 30 mg/mL PMMA (Sigma Aldrich) dissolved in chlorobenzene was spin-coated at 4000 rpm for 30 seconds onto the Gr/Cu stack. The PMMA/Gr/Cu stack was cured at 60 °C for 10 minutes. The stack was placed in 3:1 deionized (DI) H_2O:HNO_3 for 1 minute followed by DI H_2O for 1 minute to remove graphene from the back of the foil. This was repeated twice. The Cu foil was then dissolved in a solution of 0.5 M ammonium persulfate (APS) for a total of 21 hours. The PMMA/graphene film was then transferred onto a 300 nm SiO_2/Si wafer. Before transfer, the wafer was cleaned with methanol, acetone, and DI water. The Gr/SiO_2 was left to air dry for 30 minutes and was then heated to 180 °C for 5 minutes. Following this process, PMMA was dissolved in acetone. The samples were then annealed in ultra-high vacuum at 350-410 °C for three hours to remove PMMA residues. Following the anneal, the wafer was diced into smaller pieces to make a sample set for each experiment. This minimizes any variability that might exist between separately transferred samples.

Compositional Analysis of Ti

X-ray photoelectron spectroscopy of the Ti 2*p* core level was used to quantify the composition of oxide and metal components. The spectra were fit using kolXPD software.[16] An example fit is shown in Figure S1 where the metal peaks are fit with a Doniach-Sunjic lineshape convoluted with a Gaussian, and the oxide peaks are fit with a

Voigt lineshape. The integrated areas, or amplitudes, of the 2*p* core level peaks corresponding to metal (I_{metal}) and oxide (I_{oxide}) are used to calculate % oxide as follows:

$$\%\ oxide = \frac{I_{oxide}}{I_{oxide} + I_{metal}} \times 100$$

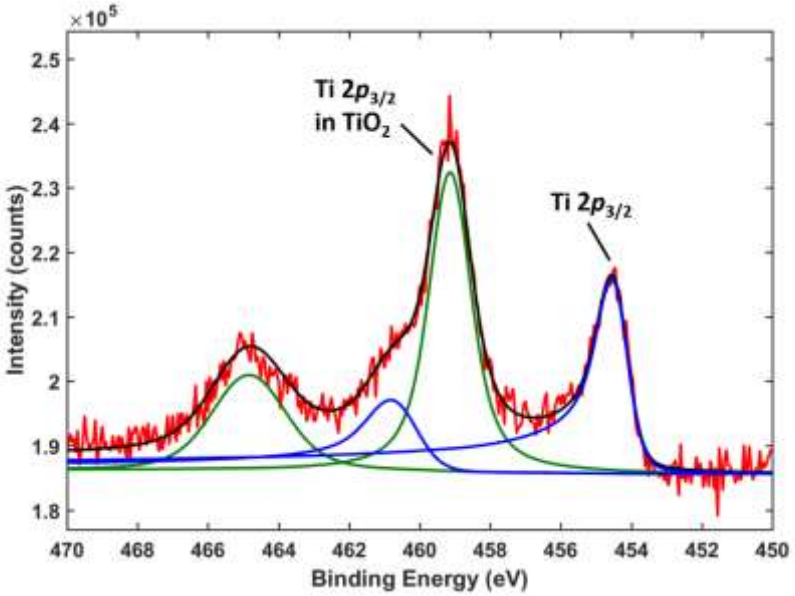

Figure S2. Example of peak deconvolution of a Ti 2*p* spectrum for Ti deposited on Gr/SiO_2 (base pressure 1x10^{-7} Torr, 0.01 nm/s deposition rate for this particular sample)

Evidence of PMMA Residue

The presence of PMMA residue is evident in XPS and Raman spectra acquired before and after annealing the transferred graphene. The XPS spectrum in Figure S3 shows the spectra components from PMMA residue, similar to the results reported by Pirkle et al in Ref. [23]. Figure S3 indicates a reduction in in polymeric species following the anneal; however, it is clear that residue remains.

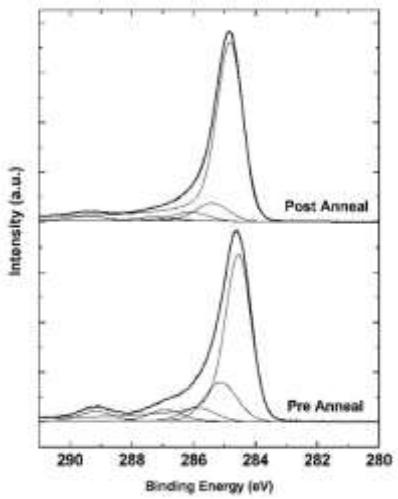

Figure S3. XPS spectra acquired before and after annealing in UHV.

The Raman spectra in Figure S4 shows an increase in the D-peak and a broadening of the G-peak following the anneal. This is consistent with results reported by Gong et al.in Ref. [44]

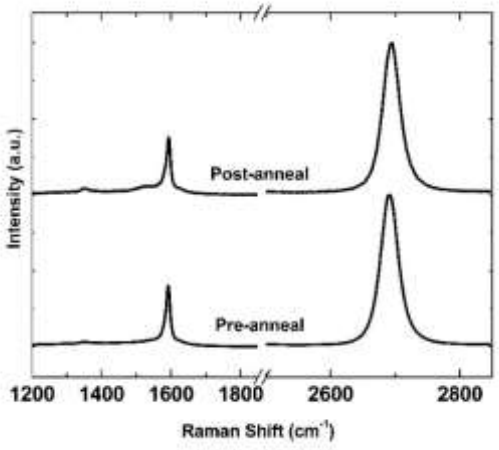

Figure S4. Raman spectra acquired with 514 nm laser before and after annealing in UHV.

Transfer Length Measurements

TLM data was acquired using 19 micron gold-plated tungsten probe tips (CascadeMicrotech, 154-001) in a probe station (JmicroTechnology, LMS-2709) connected to a SourceMeter unit (SMU, Keithley Instruments 2612A) with an applied source current of 1 mA. The data was acquired under ambient conditions within 12 to 14 days of the initial graphene transfer and within one week of contact deposition. Prior to measurement, the samples were stored in a desiccator. On each sample, sixteen TLM structures were measured and the resistances corresponding to each contact separation distance were averaged. Results acquired on the same samples after six months of air exposure show a trend consistent with the original analysis. The contact resistance of the interface was determined by plotting average contact resistance vs. separation distance and extrapolating the y- intercept from a linear fit to the data. Other graphene TLM studies utilize a wide range of TLM geometries typically processed by photolithography with contact spacings less than 100 μm.[5, 6, 45, 46] Typical reactor base pressures and deposition rates were not report and no detailed comparison with these reports in possible. The present work reports on the effect of metal deposition conditions on contact resistance and the minimization of potential variations induced by photoresist residue was therefore avoided by using a shadow mask. The impact of resist residues on contact resistance will be the focus of future work. Since the contact resistance includes any contribution to resistance that is independent of the channel length[5], resistances within the Au and Ti layers, and at the Au/TiO_x and graphene/TiO_x interfaces are all contributors to the measured value.

The TLM structure fabricated in this work, described previously by Foley *et al*[9], is shown in Figures S5.

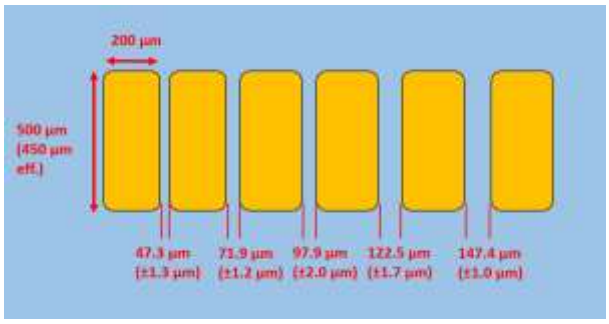

Figure S5. Top view of TLM structure

Time-Domain Thermoreflectance Measurements

Thermal boundary conductance was measured using time-domain thermoreflectance (TDTR). Laser pulses emanate from a Ti:Sapphire oscillator with an 80 MHz repetition rate,

which are energetically split into a pump path (that provides the heating event for the sample) and probe path (that is time-delayed in reference to the pump pulses) that is used to monitor the thermoreflectance of the sample under consideration as a function of pump-probe time delay. The pump path is modulated at 10 MHz and a lock-in amplifier is utilized to monitor the ratio of the in-phase to out-of-phase signal of the reflected probe beam ($-V_{in}/V_{out}$) at the pump modulation frequency for a total of 5.5 ns after the initial heating event. Several TDTR scans are performed at different locations across the samples to ensure repeatability of the measurements, and the data are fit with a model that accounts for thermal diffusion in a two layer system by fitting for h_K across the Au/SiO_2 interface.

The value of h_K provides a quantitative metric for the efficacy with which energy is exchanged across interfaces.[40] Note, in practice these reported values represent the thermal boundary conductance across an Au/SiO_2 contact with contributions from the Ti and graphene layers and contaminant interfaces. These measured Au/SiO_2 thermal boundary conductance values represent a lumped conductance value that accounts for heat flow from the Au, across the Au/Ti interface, through the Ti layer, across the Ti/Gr interface, and finally across the Gr/SiO_2 interface. Due to the relatively small thicknesses of the Ti and graphene, this Ti/Gr layer is treated as the interfacial layer between the Au and SiO_2, and thus these values for h_K are indicative of the thermal conductance across an Au/SiO_2 contact with Ti/Gr in between, consistent with prior TDTR analyses and descriptions on similar systems.[9, 22] The appropriate analysis procedure to measure h_K and the details of the experimental setup are given elsewhere.[47] The specific assumptions in our analysis regarding similar $Au/Ti/Gr/SiO_2$ systems are outlined in detail in our previous work.[9]

The time domain thermoreflectance results for all four samples represented in Figure

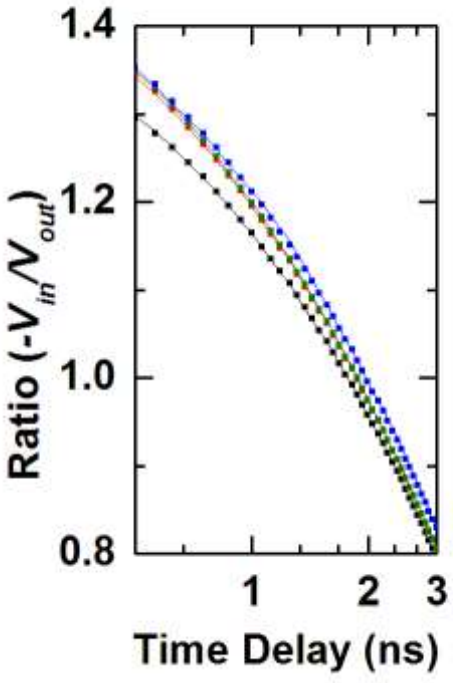

4(a) in the text is shown here in Figure S6.

Figure S6. Time-domain thermoreflectance data corresponding to Gr/SiO_2 samples with Ti deposited at different rates. The black curve is 0.01 nm/s, the blue curve is 0.05 nm/s the green curve is 0.1 nm/s and the red curve is 0.5 nm/s.

Transfer #	Base Pressure	Deposition Rate (nm/s)	Thickness of Au Capping	% Oxide	Contact Resistance	Thermal Boundary

Summary of Results

All samples included in Figure 3 of the main text are summarized in Table S1 below.

Table S2. Summary of Samples

	(Torr)		Layer (nm)		(Ω-μm)	Conductance (MW m^{-2} K^{-1})
1	1E-7	0.01	1.8	84	4.0	32
1	1E-7	0.05	2.0	27	5.0	39
1	1E-7	0.1	1.8	18	4.0	65
1	1E-7	0.5	1.6	20	2.6	58
2	1E-7	0.01	1.4	46	2.2	
2	1E-7	0.1	1.6	28	3.4	
2	1E-7	0.5	1.6	21	3.0	
3	1E-7	0.01	1.8	67	4.8	
3	1E-7	0.1	2.1	25	3.6	
3	1E-6	0.1	1.7	78	10	
3	1E-7	0.5	1.8	50	7.4	
4	1E-7	0.01	1.0	89	9.0	
4	1E-7	0.5	1.0	85	7.0	

Coefficient of Linear Correlation for R_C vs. Oxide Composition

The extent which there exists a linear correlation between a set of points $(x_1,y_1)\ldots(x_N,y_N)$, is measured by the linear correlation coefficient, *r*, given by[21]

$$r = \frac{\sigma_{xy}}{\sigma_x \sigma_y} \qquad \text{(Eq. 1)}$$

where σ_{xy} is the covariance, and σ_x and σ_y are the standard deviations of *x* and *y*. Eq. 1 can then be written as

$$r = \frac{\sum(x_i-\bar{x})(y_i-\bar{y})}{\sqrt{\sum(x_i-\bar{x})^2 \sum(y_i-\bar{y})^2}} \qquad \text{(Eq. 2)}$$

If all points (x_i,y_i) lie exactly on the line $y_i = A + Bx$ then the value of *r* will be ± 1. The quantitative significance of *r* depends on the number of measurements, *N*, which determines the probability that two *uncorrelated* variables will yield a particular value of *r*. This can be applied conversely to determine the probability that a particular value of *r* indicates that two variables are *correlated*. For the data reported in this work plotted in Figure 1 of the text, the measurement of oxide composition and R_C on thirteen distinct samples yielded a correlation coefficient of 0.7. By the methods reported in Ref. 1, this represents a 0.8% probability that oxide composition and R_C are *uncorrelated*. We therefore infer a 99.2% probability that R_C is linearly correlated with oxide composition. This value corresponds to a *highly significant* probability of linear correlation.